

The formation of a detached shell around the carbon star Y CVn

Y. Libert¹, E. Gérard² and T. Le Bertre¹

¹LERMA, UMR 8112, Observatoire de Paris, 61 av. de l'Observatoire, F-75014 Paris, France

²GEPI, UMR 8111, Observatoire de Paris, 5 place J. Janssen, F-92195 Meudon Cedex, France

Accepted 2007 June 25. Received 2007 June 18; in original form 2007 April 6

ABSTRACT

Y CVn is a carbon star surrounded by a detached dust shell that has been imaged by the *Infrared Space Observatory* at 90 μm . With the Nançay Radio Telescope we have studied the gaseous counterpart in the 21-cm H I emission line. New data have been acquired and allow to improve the signal to noise ratio on this line. The high spectral resolution line profiles obtained at the position of the star and at several off-set positions set strong constraints on the gas temperature and kinematics within the detached shell; the bulk of the material should be at $\sim 100\text{--}200$ K and in expansion at $\sim 1\text{--}2$ km s^{-1} . In addition, the line profile at the central position shows a quasi-rectangular pedestal that traces an 8 km s^{-1} outflow of $\sim 1.0 \cdot 10^{-7} M_{\odot} \text{yr}^{-1}$, stable for about $2 \cdot 10^4$ years, which corresponds to the central outflow already studied with CO rotational lines.

We present a model in which the detached shell results from the slowing-down of the stellar wind by surrounding matter. The inner radius corresponds to the location where the stellar outflow is abruptly slowed down from ~ 8 km s^{-1} to 2 km s^{-1} (termination shock). The outer radius corresponds to the location where external matter is compressed by the expanding shell (bow shock). In this model the mass loss rate of Y CVn has been set constant, at the same level of $1.0 \cdot 10^{-7} M_{\odot} \text{yr}^{-1}$, for $\sim 4.5 \cdot 10^5$ years. The gas temperature varies from ~ 1800 K at the inner limit to 165 K at the interface between circumstellar matter and external matter.

Our modelling shows that the presence of a detached shell around an AGB star may not mean that a drastic reduction of the mass loss rate has occurred in the past. The inner radius of such a shell might only be the effect of a termination shock rather than of an interruption of the mass loss process.

Key words: stars: AGB and post-AGB – stars: carbon – (stars:) circumstellar matter – stars: individual: Y CVn – stars: mass-loss – radio lines: stars.

1 INTRODUCTION

The history of the mass loss experienced by stars on the Asymptotic Giant Branch (AGB) is a key issue for describing the late stages of evolution of low and intermediate mass ($1\text{--}6 M_{\odot}$) stars, as well as an important ingredient for the characterization of the cosmic cycle of matter. Determining the mass loss rates of red giants is generally based on modelling radio molecular line profiles (Schöier 2007) or infrared continuum energy distributions (van Loon 2007). However these methods are limited to the central parts of circumstellar shells, and, as the mass loss rates of AGB stars are variable, it has been difficult to establish a balance of the mass loss over the long periods of time that need to be considered ($10^4\text{--}10^6$ years).

In principle the H I line at 21 cm should be a useful tracer of AGB circumstellar environments (Le Bertre et al.

2005). Hydrogen dominates their composition (~ 70 % in mass) and should be in atomic form, at least in the external parts of these shells ($r \geq 0.1$ pc). However the 21 cm line is weak and generally contaminated by the much more intense galactic emission arising on the same lines of sight. H I line observations of AGB stars have long been limited to Mira (Bowers & Knapp 1988). However, since 2001, using the upgraded Nançay Radiotelescope (NRT), we readdressed this issue and detected several objects in emission, in particular RS Cnc (Gérard & Le Bertre 2003), EP Aqr & Y CVn (Le Bertre & Gérard 2004, Paper I), and X Her (Gardan et al. 2006, Paper II). Recently, we also presented the results of a survey of 22 sources, with 18 new detections (Gérard & Le Bertre 2006, Paper III). Using the Very Large Array (VLA), Matthews & Reid (2007) detected H I emission coincident in both position and velocity with RS Cnc, and

reported emission close to, but not unambiguously related to, EP Aqr. They also reported H I emission from the circumstellar shell of R Cas.

Generally the H I emissions that we detect with the NRT are extended, indicating shell sizes ~ 1 pc. In some cases, e.g. EP Aqr (Paper I), they reveal complex spatial and dynamic structures. The 21 cm line thus probes regions much larger than those that can be studied with molecular lines, which are limited by photo-dissociation ($r \leq 0.1$ pc). Extended shells have also been observed in the far-infrared continuum emission (60 and 100 μm) by the Infrared Astronomical Satellite (IRAS, Young et al. 1993a). The spatial extension estimated from our H I observations are comparable to, or possibly larger than, those obtained by Young et al. (1993a). Some of the infrared shells appeared detached from the central stars. The infrared source associated to Y CVn was reobserved by the *Infrared Space Observatory* (ISO), which clearly detected at 90 μm a detached dust shell surrounding the central star (Izumiura et al. 1996). These detached shells were interpreted as resulting from the interaction of the expelled material with the Interstellar Medium (ISM, Young et al. 1993b), or from a past event of mass loss much higher than today (Izumiura et al. 1996). However the far-infrared data lack crucial kinematic information.

The H I line profiles obtained with the NRT have in general a gaussian shape, with a Full Width at Half-Maximum (FWHM) smaller than, or equal to, the width of the CO rotational lines, implying that the expansion velocity decreases outward (Papers I & III). This slowing-down of the outflows indicates an interaction with local material, either of circumstellar or interstellar origin. These high-spectral-resolution H I profiles provided the first direct evidence of a slowing-down of circumstellar matter in the external shells of red giants.

In the present paper, we revisit the case of Y CVn, because, as the ISO observations show images that are rather rounded, we expect that a spherical symmetry may apply and therefore that the interpretation will be easier. Also the source is relatively bright in H I, with a low interstellar contamination, so that in principle H I profiles of high quality are accessible. With these favorable conditions we expect that the H I profile modelling will bring useful constraints on the detached shell characteristics, and more generally on the detached shell phenomenon. We have acquired new H I data on Y CVn in order to improve those already presented in Paper I.

2 Y CVN

2.1 The central star

Y CVn is a J-type carbon star, i.e. a carbon star whose photosphere is enriched in ^{13}C . The abundance ratio, $^{12}\text{C}/^{13}\text{C} \sim 3.5$ (Lambert et al. 1986), is close to the CNO-cycle equilibrium value (3-3.5, Lattanzio & Forestini 1999). The effective temperature is ~ 2760 K (Bergeat et al. 2001), so that atomic hydrogen should dominate over molecular hydrogen in the atmosphere and eventually above it (Glassgold & Huggins 1983). However, Lambert et al. (1986) detected a weak 1-0 S(0) H₂ line at 2.22 μm , so that some hydrogen should still be in molecular form within the photosphere.

The abundance analysis performed by Lambert et al. shows also that Y CVn may have a slightly sub-solar metallicity (-0.2 ± 0.2), with oxygen showing the most underabundance (-0.4).

The exact stage of evolution of Y CVn is not clear. J-type stars do not show an enhancement in s-process elements, suggesting that they have not gone through thermal pulses and that the surface carbon enrichment is not due to a third-dredge-up event. For instance, they might owe their carbon-rich composition to an He core flash when they were still on the Red Giant Branch (Dominy 1984).

The distance derived from the *Hipparcos* parallax (4.59 ± 0.73 mas, Perryman et al. 1997) is ~ 218 pc. This places Y CVn at 207 pc from the Galactic Plane in a direction close to the Galactic North pole ($b^{\text{II}} = 72^\circ$). We adopt the *Hipparcos* distance, but note that it might be underestimated. Knapp et al. (2003) have re-reduced the *Hipparcos* data and give a revised parallax (3.68 ± 0.83 mas) that tends to place the source somewhat further from the Sun (272 pc). Also Bergeat et al. (2002) estimate the parallax at ~ 3.85 mas (or ~ 260 pc).

The K magnitude is -0.74 (Guandalini et al. 2006) which translates to a bolometric magnitude of 1.96 (Le Bertre et al. 2001) or $\sim 6200 L_\odot$ at 218 pc. Such a luminosity places Y CVn clearly on the AGB, probably on the early AGB (E-AGB) rather than on the thermally pulsing AGB (TP-AGB).

The proper motion observed by *Hipparcos* is -2.20 , in Right Ascension (RA), and $13.05 \text{ mas yr}^{-1}$, in Declination. When corrected for the solar motion towards apex, it translates to 13.4 and 17.4 mas yr^{-1} respectively, and for a distance of 218 pc to 14 and 18 km s^{-1} , with respect to the (solar) Local Standard of Rest (LSR). It corresponds to a motion, in the plane of the sky, towards North-East (position angle, $\text{PA} = 38^\circ$).

2.2 The circumstellar envelope

Evidence for the presence of a circumstellar shell around Y CVn was found by Goebel et al. (1980) who detected the $11.3\text{-}\mu\text{m}$ band ascribed to SiC dust grains. The 1-0 rotational line of CO was first detected by Knapp & Morris (1985).

Knapp et al. (1998) have obtained a high-resolution CO spectrum of the wind from Y CVn. They determine a LSR radial velocity, $V_{\text{LSR}} = 21.1 \text{ km s}^{-1}$, an expansion velocity, $V_{\text{exp}} = 7.8 \text{ km s}^{-1}$, and a mass loss rate, $\dot{M} = 1.1 \cdot 10^{-7} M_\odot \text{ yr}^{-1}$ (at 218 pc). Schöier et al. (2002) obtained similar estimates with $V_{\text{exp}} = 8.5 \text{ km s}^{-1}$ and $\dot{M} = 1.5 \cdot 10^{-7} M_\odot \text{ yr}^{-1}$, as well as Teyssier et al. (2006) with $V_{\text{exp}} = 6.5 \text{ km s}^{-1}$ and $\dot{M} = 1.0 \cdot 10^{-7} M_\odot \text{ yr}^{-1}$. The CO emission is extended with diameters, $\phi \sim 13''$ in the 1-0 transition, and $\sim 9''$ in 2-1 (Neri et al. 1998). A faint asymmetry is suspected in the 2-1 data.

An intense emission in the ^{13}CO 1-0 line, detected by Jura et al. (1988), confirms the large abundance of ^{13}C in the Y CVn outflow. Schöier & Olofsson (2000) evaluate the $^{12}\text{CO}/^{13}\text{CO}$ abundance ratio to ~ 2.5 , a ratio larger than the equilibrium value, indicating a possible enrichment in ^{13}C of the CO molecule within the outflow. The mass loss rates estimated from ^{12}CO rotational line data may therefore be underestimated by a factor ~ 1.4 . We note also that the underabundance in oxygen, as suggested by Lambert et al.

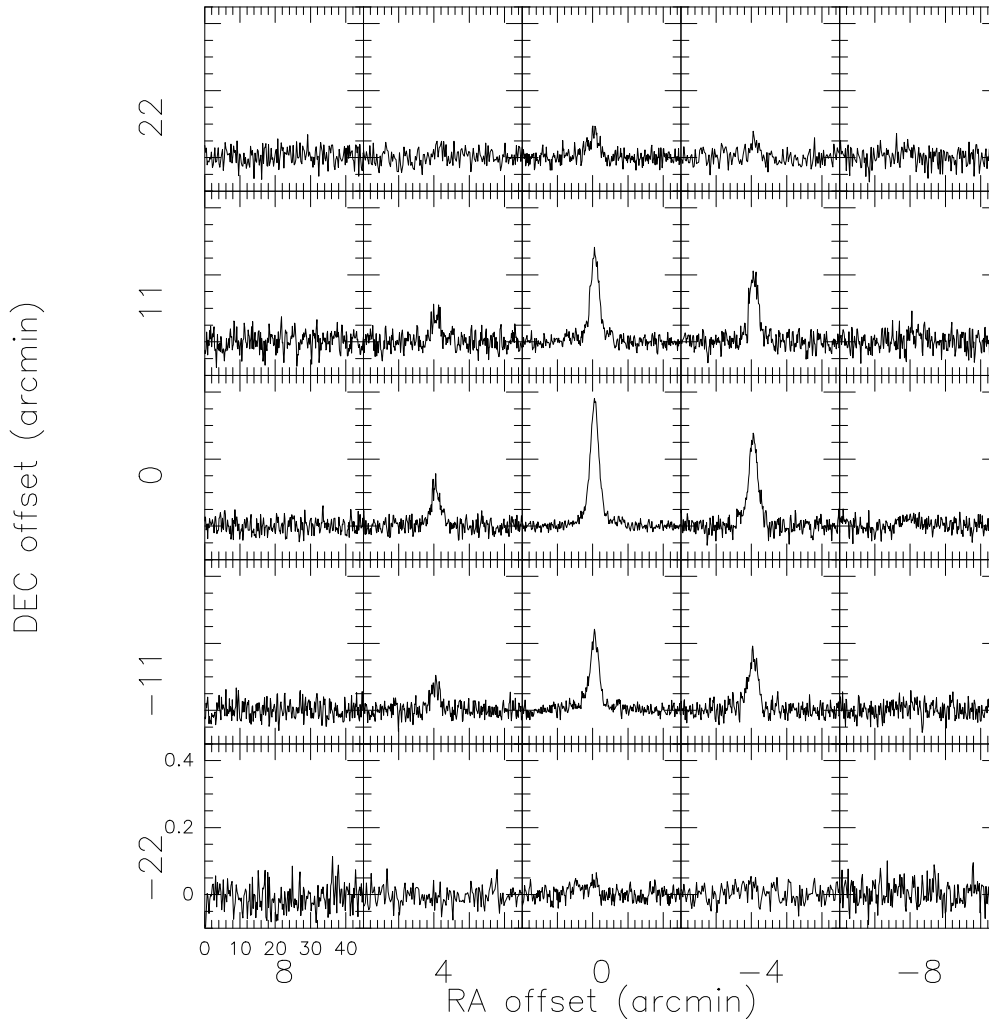


Figure 1. Map of the 21 cm HI emission from the Y CVn circumstellar envelope observed with the NRT. The steps are $4'$ in RA (1 beam) and $11'$ in Declination ($1/2$ beam). North is up and East to the left.

(1986), would directly translate into an underabundance in CO.

An extended emission at 60 and 100 μm was discovered by IRAS (Young et al. 1993a). This emission could be modelled with a resolved isothermal shell, at $\sim 30\text{-}40$ K, of inner radius, $r_{in} \sim 2.8'$, and outer radius, $r_{out} \sim 5.5'$. An image at 90 μm with a better spatial resolution ($\sim 40''$) and a better sensitivity was obtained by ISO (Izumiura et al. 1996). It clearly shows a central infrared source surrounded by a quasi-circular detached shell, with $r_{in} \sim 2.8'$ and $r_{out} \sim 5.1'$. This image of a detached shell supports the modelling of the IRAS data by Young et al. (1993a). In addition, in the ISO image at 90 μm , the detached shell seems displaced to the West by about $0.5\text{-}1'$ with respect to the central infrared source. Nevertheless, the circular morphology of the detached shell and the small size of the offset, as compared to the source diameter, leave no doubt on the association with Y CVn. Adopting a *dust-to-gas* mass ratio of $4.5 \cdot 10^{-3}$, the mass in the detached shell can be estimated at $0.06 M_{\odot}$ (at 218 pc).

This detached shell, observed in the dust continuum emission, is interpreted by Young et al. (1993b) as a product of the slowing-down of an expanding circumstellar shell by the surrounding ISM. On the other hand, for Izumiura et al. (1996), it is the result of an intense episode of mass loss, about two orders of magnitude larger than presently (as probed by the CO emission, which is limited to the central $\sim 10''$, Neri et al. 1998), with an outflow velocity $\sim 15 \text{ km s}^{-1}$, that lasted about $2 \cdot 10^4$ years and stopped $1.4 \cdot 10^4$ years ago.

In Paper I, we reported the detection of Y CVn in the HI line at 21 cm. The emission is extended compared to the NRT beam size in Right Ascension ($4'$). The line profile is composite with a spectrally narrow component (Comp. 1, $\text{FWHM} \sim 2.9 \text{ km s}^{-1}$) superposed on a weak broad component (Comp. 2, $\text{FWHM} \sim 14 \text{ km s}^{-1}$). The 2 components are centered at $V_{\text{lsr}} \sim 20\text{-}21 \text{ km s}^{-1}$, in good agreement with the CO lines. Comp. 1 was found to be spatially extended ($\sim 12'$) and to be more intense West than East. The HI source traced by Comp. 1 was associated to the detached

shell observed by ISO, whereas the other one was associated with the Y CVn outflow already observed in CO molecular lines.

The spatially extended emission associated to Comp. 1 and its quasi-gaussian line-profile of width $\sim 3 \text{ km s}^{-1}$ were interpreted as an indication that the outflow velocity should decrease outward, a result which agrees with the Young et al. (1993b) interpretation of a slowing-down by the surrounding ISM. However it does not exclude a brief episode of a large mass loss rate in the past (see Sect. 6).

3 OBSERVATIONS

The NRT has a rectangular aperture of effective dimensions $160 \text{ m} \times 30 \text{ m}$. At 21 cm, its beam has a FWHM of $4'$ in Right Ascension (RA) and $22'$ in Declination. The data on Y CVn have been acquired in the position-switch mode with off-positions taken at $\pm 4'$, $\pm 8'$, $\pm 12'$, $\pm 16'$, and $\pm 32'$ from the central position in the East-West direction. The central positions were selected on the position of the star (adopted from the SIMBAD database: $12^{\text{h}}45^{\text{m}}07.8^{\text{s}} + 45^{\circ}26'25''$, 2000.0), and at $\pm 11'$ and $\pm 22'$ from it, in the North-South direction. The spectral resolution corresponds to 0.32 km s^{-1} . For more details we refer to Paper I.

In order to obtain the best H I line profiles needed for our modelling, we have re-processed our previous data with an improved procedure (better weighting of the individual observations) and acquired new observations, with a bandwidth twice as large, allowing a better determination of the baselines. In total, 107 hours of data have been acquired between Sept. 2002 and Jan. 2007, and are used in the present work.

The new map, that results from the merging of old and new data (Fig. 1), has a much better quality than the one presented in Paper I. The signal-to-noise ratio is on average twice better than in our 2004 map (Paper I).

The H I line at the stellar position (full line in Fig. 2) is clearly dominated by a narrow quasi-gaussian component (Comp. 1) of FWHM $\sim 3.1 \text{ km s}^{-1}$, and intensity $\sim 360 \text{ mJy}$, superposed on a weak rectangular pedestal of width $\sim 16 \text{ km s}^{-1}$, and intensity $\sim 10 \text{ mJy}$. In Table 1 we give the results of the line fitting by the sum of a gaussian and of a rectangle; as this fitting closely matches the data, it is not represented in the figures. The dashed lines result from the modelling of the whole map that will be discussed in Sect. 5. The radial velocities of the two components are nearly the same and in agreement, within 0.5 km s^{-1} , with that of Y CVn as determined from CO data (Knapp et al. 1998). The improved quality of our H I spectrum allows to see that Comp. 2 might have a rectangular profile rather than a gaussian one (cf. Paper I); nevertheless, for continuity, we keep the same notation, Comp. 1 & 2, as in Paper I.

East and West of the central position (Fig. 3, upper panel) the H I line profile is essentially gaussian-like, i.e. with the present signal-to-noise ratio we do not detect a pedestal. We confirm the asymmetry between East and West, which is consistent with that seen on the ISO image at $90 \mu\text{m}$. From the relative fluxes of Comp. 1 between the central position and the two offset positions, we estimate the displacement at $\sim 1'$ West. As noted in Sect. 2.1, this displacement is small

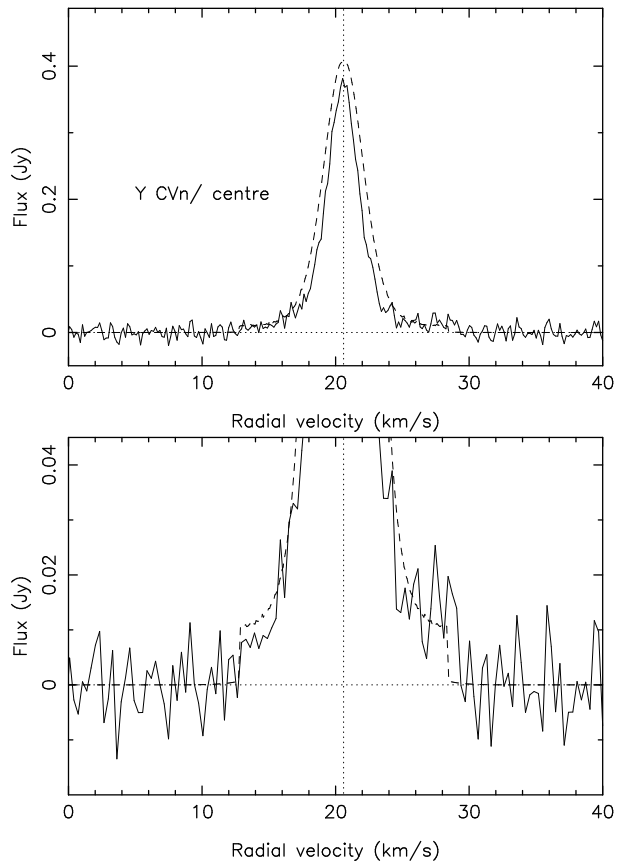


Figure 2. H I spectrum obtained with the NRT on the stellar position (thin line) and modelled spectrum (Sect. 5; dashed line). A zoom on the lower part of the spectrum is displayed in the lower panel in order to show better the pedestal (Sect. 3). The vertical dotted line indicates the radial velocity adopted for the model ($V_{\text{lsr}} = 20.6 \text{ km s}^{-1}$).

Table 1. Fits to the two H I components of Y CVn (not represented in the figures). Comp. 1 is fitted with a gaussian profile, and Comp. 2 with a rectangular profile. In the case of Comp. 1 we quote the FWHM and for Comp 2 the full width. For comparison the CO (3-2) profile obtained by Knapp et al. (1998) gives $V_{\text{lsr}} = 21.1 \text{ km s}^{-1}$ and $V_{\text{exp}} = 7.8 \text{ km s}^{-1}$.

	V_{cent} km s^{-1}	Width km s^{-1}	F_{peak} mJy
Comp. 1 (center)	20.5	3.1	358.
Comp. 2 (center)	21.1	15.6	10.
Comp. 1 ($\pm 4'$ in RA)	20.5	3.2	179.
Comp. 1 ($\pm 11'$ in Dec.)	20.6	3.1	232.
Comp. 1 ($\pm 11'$ in Dec. and $\pm 4'$ in RA)	20.5	3.2	132

compared to the source size. In addition, we note that the radial velocity of Comp. 1 is consistent with that of Y CVn further supporting their association. We do not detect the source at $\pm 8'$ from the stellar position (Fig. 3, lower panel). The diameter of the H I source can then be estimated at $8' \pm 4'$.

The source is clearly detected at $\pm 11'$ in the North-South direction (Fig. 4, upper panel) with more than half the

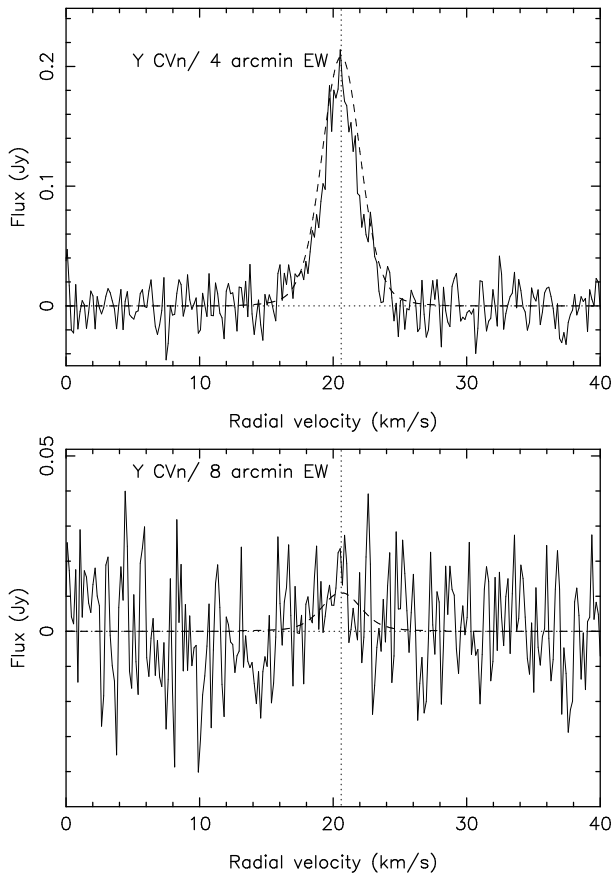


Figure 3. Upper panel: average H I spectrum obtained with the NRT on the two off-positions at $\pm 4'$ in RA (thin line) and modelled spectrum (Sect. 5; dashed line). Lower panel: same, with the two off-positions at $\pm 8'$.

flux on Y CVn. Therefore it is also extended in Declination, but our spatial resolution is not sufficient to characterize the size in this direction. In the map, we note that the source is slightly more intense North than South, by about 10 % at $\pm 11'$, which is an indication of a slight (relative to the beam) displacement North that we estimate at $1' \pm 0.5'$. Finally, the source is also detected at the four positions $\pm 4'$ in RA and $\pm 11'$ in Declination (Fig. 4, lower panel).

By integrating the line profiles over the full map, the total H I flux associated to Y CVn can be estimated at $3.38 \text{ Jy km s}^{-1}$. At 218 pc, this translates to $3.8 \pm 0.2 \cdot 10^{-2} M_{\odot}$ in atomic hydrogen. Most of it is associated to Comp. 1. We estimate the flux corresponding to Comp. 2, from the width and height of the pedestal detected on the Y CVn position, at $0.16 \text{ Jy km s}^{-1}$, or $1.8 \cdot 10^{-3} M_{\odot}$.

4 INTERPRETATION

Although we are limited by the spatial resolution of the NRT ($4' \times 22'$), by combining our high-spectral resolution H I data with the ISO image obtained in the dust continuum by Izumiura et al. (1996), we can obtain a description of the Y CVn circumstellar environment that takes into account the kinematics of the gas.

The source traced by Comp. 2 can be associated with

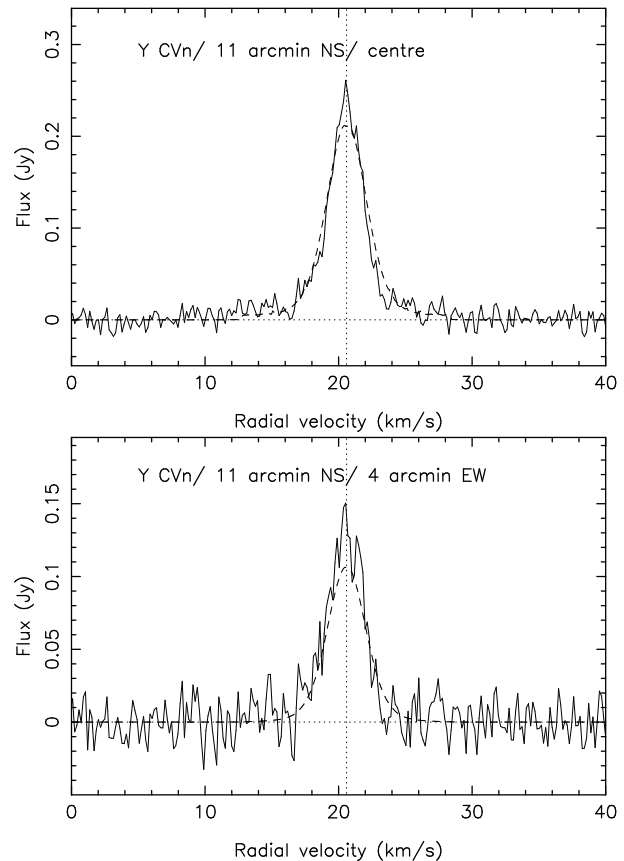


Figure 4. Upper panel: average H I spectrum obtained with the NRT on the two positions at $\pm 11'$ in Declination (thin line) and modelled spectrum (Sect. 5; dashed line). Lower panel: same, with the four off-positions at $\pm 11'$ in Declination and $\pm 4'$ in RA.

the central infrared source. Its rectangular profile is typical of an optically thin H I emission of a uniformly expanding shell (Paper I). The expansion velocity ($\sim 8 \text{ km s}^{-1}$) is consistent with the outflow velocity obtained from CO rotational lines. As Comp. 2 is also centered on the radial velocity of Y CVn, we can infer that the corresponding source has a nearly spherical geometry.

The source traced by Comp. 1 is spatially resolved by the NRT and has a diameter, $\phi \sim 8' \pm 4'$. Its hydrogen mass is consistent with the total mass of the detached shell estimated by Izumiura et al. (1996). Therefore it is reasonable to associate it to the infrared detached shell. The spectral width, $\sim 3 \text{ km s}^{-1}$, shows that the material is moving outwards at a reduced velocity as compared to the source traced by Comp. 2. This is in agreement with the analysis of Young et al. (1993b).

We now pursue this analysis and consider the interaction of the Y CVn outflow with external matter. The infrared image and our H I map show an offset of $1'$ West with respect to the central source, but this offset is small compared to the diameter of the detached shell, and in the ISO image the detached shell has a quasi-circular appearance. Also the central velocity in H I (20.6 km s^{-1}) is close to that in CO (21.1 km s^{-1}), so that no large deviation along the line of sight can be detected. In the following we assume spherical symmetry, which in particular implies that the external medium is at rest with respect to Y CVn.

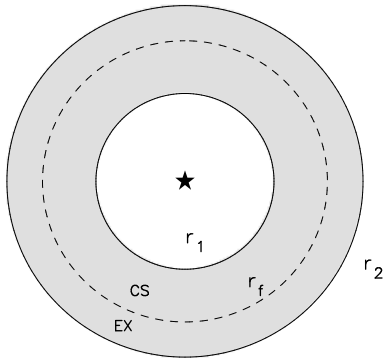


Figure 5. Schematic view of the Y CVn detached shell. The termination shock is located in r_1 , the contact discontinuity in r_f , and the bow shock in r_2 . CS stands for circumstellar material and EX, for external material (see Sect. 4).

The interaction of a spherical outflow with external matter leads to the formation of a region of compressed material within two spherical boundaries (Fig. 5; Lamers & Cassinelli 1999). The internal boundary, r_1 , defines the surface at which the supersonic outflow is abruptly slowed-down by compressed circumstellar material (termination shock). The external boundary, r_2 , defines the surface at which the external medium is compressed by the expanding shell (bow shock). Within these two limits we find compressed materials of stellar (CS) and external (EX) origins that are separated by a contact surface defined by r_f . In this description no material is allowed to flow over the contact discontinuity in r_f . Finally, inside r_1 , the stellar outflow is in free expansion.

We interpret the detached shell observed by ISO and the H I source traced by Comp. 1 as this region of compressed material delineated by r_1 and r_2 , and identify r_1 with r_{in} and r_2 with r_{out} . I.e. we assume that the dust and the gas have a similar spatial distribution; this assumption is further discussed in Sect. 6. We also adopt the best estimates from Izumiura et al. (1996), so that for a distance of 218 pc, $r_1 = 0.18$ pc, and $r_2 = 0.32$ pc.

The width of the H I emission allows to estimate an upper limit to the average H I temperature within the compressed shell. For a maxwellian distribution of hydrogen atoms at temperature T , the H I emission projected on a line of sight has a gaussian profile of width (Gérard 1990):

$$FWHM(km s^{-1}) = 0.214(T(K))^{1/2} \quad (1)$$

Therefore, the temperature of the gas within the detached shell is, on average, at most 210 K. Conversely, the bulk of the material in the detached shell is moving outwards at a maximum velocity $\sim 1/2$ FWHM, i.e. ~ 2 km s $^{-1}$.

The source associated to Comp. 2 can be identified with the freely flowing stellar wind that fills the region inside the termination shock ($r < r_1$). The crossing time is about $22 \cdot 10^3$ years, which translates to an average mass loss rate in atomic hydrogen of about $0.8 \cdot 10^{-7} M_{\odot} yr^{-1}$.

The atomic hydrogen mass of the detached shell, M_{DT} = $3.6 \cdot 10^{-2} M_{\odot}$, can be separated in two components: a circumstellar part, $M_{DT,CS}$, located between r_1 and r_f , and an external one, $M_{DT,EX}$, between r_f and r_2 (see Fig. 5). To es-

timate the latter we assume that it is equal to the hydrogen ISM mass enclosed in a sphere of radius r_2 . Following Young et al. (1993b) we adopt an ISM density of 0.25 H cm^{-3} from a galactic scale height of 100 pc, and an ISM density of 2 H cm^{-3} in the galactic plane. In these conditions, $M_{DT,EX} \sim 0.9 \cdot 10^{-3} M_{\odot}$, and therefore $M_{DT,CS}$ can be estimated at $\sim 3.5 \cdot 10^{-2} M_{\odot}$ in atomic hydrogen. The mass of the detached shell appears clearly dominated by circumstellar material. We note that Y CVn is relatively close to the Sun, in a direction for which the interstellar medium might be deficient (Sfeir et al. 1999), so that we might have been overestimating the ISM density.

Finally, if we assume that the mass loss rate has been constant with time, and adopt the total mass derived from Comp. 2, $M_{DT,CS}$, we obtain a characteristic time for the formation of the detached shell of $t_{DS} \sim 4.5 \cdot 10^5$ years, ~ 20 times larger than the crossing time of the freely flowing wind region. A characteristic velocity for the expansion of the detached shell is then: $r_1/t_{DS} \sim 0.4 \text{ km s}^{-1}$. This is probably an overestimate of the present expansion rate, as the expansion rate should decrease with time (Young et al. 1993b).

In conclusion the detached shell appears as a region of the Y CVn environment where circumstellar matter has been slowed down and is stored for a few 10^5 years before being injected in the ISM.

5 MODELLING

For the freely expanding wind zone ($r < r_1$), we consider an outflow with a constant velocity ($v_0 = 8 \text{ km s}^{-1}$) and a volumic density varying in $1/r^2$, corresponding to a constant hydrogen mass loss rate. The temperature of the gas is assumed to be low enough that its effect on the H I profile can be neglected. Indeed, at distances larger than 10^{16} cm the gas temperature should be lower than 100 K (e.g. Kahane & Jura 1994) and the thermal broadening should stay small compared to v_0 .

In order to describe the detached shell around Y CVn ($r_1 < r < r_2$) in simple terms, we make the hypotheses of stationarity and spherical symmetry; all quantities depend only on r , the distance to the central star, and in particular the limits r_1 , r_f and r_2 are treated as independent of time. The mass flow is constant, and the same rate apply in the detached shell from r_1 to r_f as in the freely expanding wind zone ($r < r_1$):

$$\dot{M} = 4\pi r^2 \rho v \quad (2)$$

where ρ and v are the density and velocity in r . For \dot{M} , we adopt the value corresponding to that determined in Sect. 4, $\dot{M}_{HI} = 0.8 \cdot 10^{-7} M_{\odot} yr^{-1}$.

We assume that the gas behaves as an ideal gas of mean molecular weight, μ . The pressure (p), density and temperature (T) are then related by the equation of state:

$$p = \rho \frac{kT}{\mu m_H} = \rho c^2 \quad (3)$$

where c is the isothermal sound velocity, k the Boltzmann constant, and m_H the mass of the hydrogen atom. For a neutral atomic gas with 10 per cent ^4He , and 90 per cent H, $\mu = 1.3$.

The equation of motion for an ideal gas in spherical geometry is given by :

$$v \frac{dv}{dr} = -\frac{1}{\rho} \frac{dp}{dr} = -\frac{1}{\rho} \frac{k}{\mu m_H} \frac{d\rho T}{dr} \quad (4)$$

(i.e. we neglect the stellar gravity). Using Equ. 2, which is valid from r_1 to r_f , we re-write (4) as:

$$\frac{dv}{dr} \left(v - \frac{c^2}{v} \right) = 2 \frac{c^2}{r} - \frac{k}{\mu m_H} \frac{dT}{dr} \quad (5)$$

The properties of the gas in r_1 are given by the jump conditions (Dyson & Williams 1997):

$$\rho_0 v_0 = \rho_1 v_1 \quad (6)$$

$$\frac{v_1}{v_0} = \frac{M_0^2 + 3}{4M_0^2} \approx \frac{1}{4} \quad (7)$$

where ρ_0 , v_0 and M_0 are the upstream density, velocity and Mach number. Equ. 6 is a general expression while Equ. 7 only applies to a mono-atomic adiabatic gas. From the previous discussion we adopt $v_0 \sim 8 \text{ km s}^{-1}$ and deduce ρ_0 from the mass loss rate. We estimate $M_0 \sim 20$ assuming an upstream temperature, $T_0 = 20 \text{ K}$. The downstream temperature within r_1 , T_1 , is given by:

$$T_1 \approx \frac{3\mu m_H}{16k} v_0^2 \sim 1800 \text{ K} \quad (8)$$

As the average temperature within the detached shell is at most 210 K (previous section), the gas must cool down to a temperature lower than 210 K within the time lapse of the detached shell formation ($\sim 4 \cdot 10^5$ years). This cooling should occur through atomic lines and/or dust emission, and probably depends on metallicity. (Some heating of the gas by dust may also be expected close to r_1 , see Sect. 6.) We do not estimate the cooling rate, but rather adopt a temperature profile through the detached shell that we will constrain from our H I observations. In practice we adopt a law of the form:

$$\log \frac{T}{T_1} = a \log \frac{r}{r_1} \quad (9)$$

with $T_1 = 1800 \text{ K}$. Equ. (5) can then be re-written as:

$$\frac{dv}{dr} \left(v - \frac{c^2}{v} \right) = \frac{c^2}{r} (2 - a) \quad (10)$$

The equation of motion (10) is solved layer by layer, using the classical Runge-Kutta method, outwards from r_1 , under the initial conditions of density, temperature and velocity, ρ_1 , T_1 and v_1 . The limit r_f is set such that the hydrogen mass between r_1 and r_f is equal to $M_{DT,CS}$.

From r_f to r_2 , we cannot use Equ. 5. As the amount of interstellar matter between r_f and r_2 is small compared to the mass in the detached shell, we simply assume a $1/r^2$ dependence for the density in this region, with the condition that its hydrogen mass is equal to $M_{DT,EX}$, i.e. $0.9 \cdot 10^{-3} M_\odot$. The temperature is assumed constant from r_f to r_2 (although strictly speaking it is expected to increase from r_f to r_2). The velocity is then obtained from Equ. 4.

The velocity, hydrogen-density and temperature profiles are then used in an H I emission model that we have already developed (Papers I and II). For each point within the detached shell, the thermal broadening is derived through Equ. 1. In the model the H I emission from an envelope of matter flowing radially from the central star is convolved

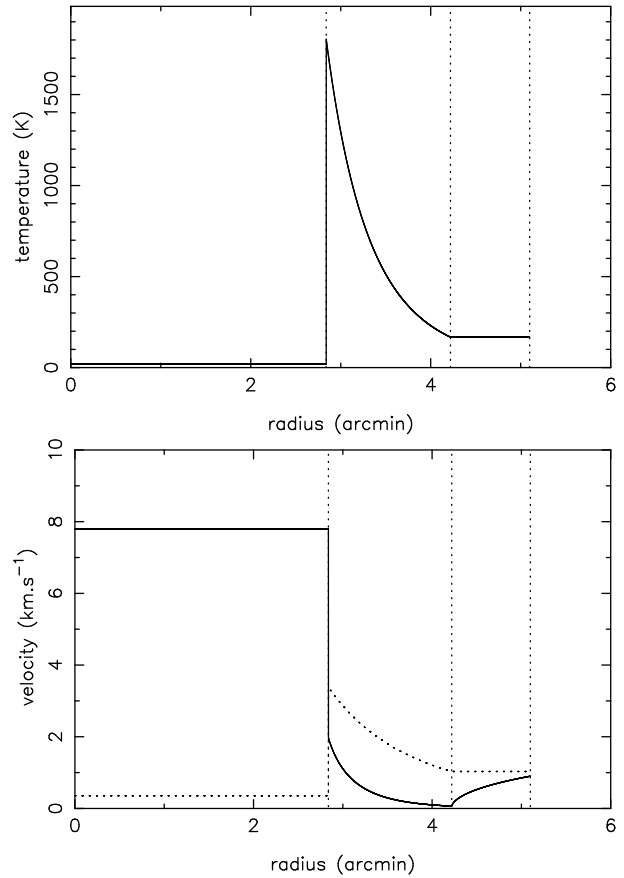


Figure 6. Upper panel: adopted temperature profile in the detached shell for the model described in Sect. 5. Lower panel: velocity profile. The dashed line represents the isothermal sound velocity (c).

with the response given by a telescope of rectangular aperture with effective dimensions $160 \text{ m} \times 30 \text{ m}$. We thus calculate the H I emission as it should be observed by the NRT at the central position and at different positions offset in RA and Declination (dashed lines in Fig. 2, 3 and 4). It should be noted that in the present modelling the temperature profile plays a double rôle, first in the kinematics through the isothermal sound velocity (Equ. 3), second in the H I profile through thermal Doppler broadening.

Our modelling depends only on the value selected for the constant a in Equ. 9. For the comparison with the observations (Fig. 2 and following) we adopted a stellar velocity, $V_{\text{lsr}} = 20.6 \text{ km s}^{-1}$. We tested several values and obtained a satisfactory fit to the observed H I line profiles for $a = -6.0$. The resulting temperature profile in the detached shell is plotted in Fig. 6 (upper panel); it reaches a minimum in r_f at $\sim 165 \text{ K}$. The corresponding velocity profile is shown in the same figure (lower panel). Within the detached shell, the flow remains sub-sonic; the velocity profile that we obtain is similar to the “breeze” solution of the classical theory of stellar winds (e.g. Lamers & Cassinelli 1999). The density profile and the flux of matter are shown in Fig. 7. Both are clearly peaked at $r_f = 0.27 \text{ pc}$ ($4.22'$).

The numerical values used for the parameters of the model are summarized in Table 2.

The H I emission model developed in Papers I and II

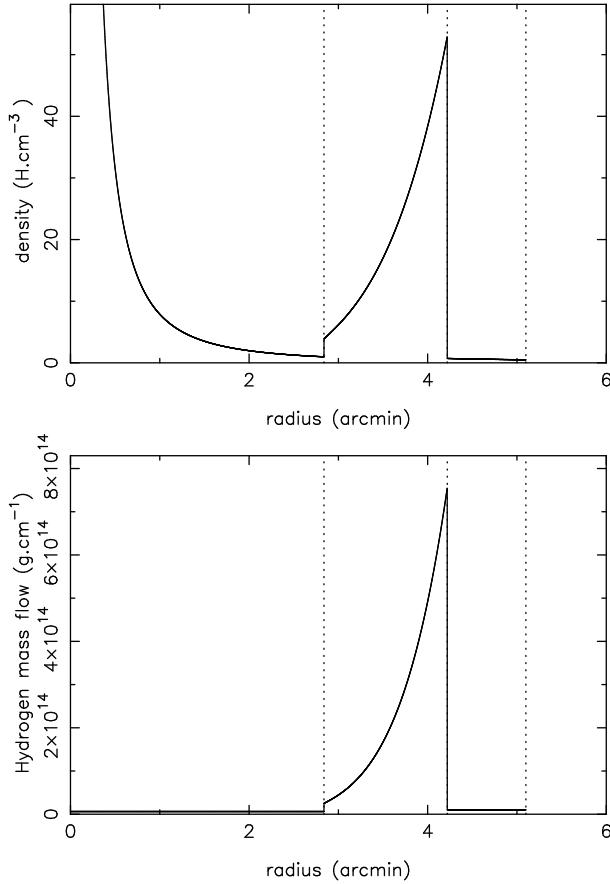


Figure 7. Upper panel: atomic hydrogen density profile for the model described in Sect. 5. Lower panel: atomic hydrogen mass-flow profile. The vertical dotted lines mark the radii, r_1 , r_f and r_2 , of the model.

assumes that the brightness temperature is proportional to the atomic hydrogen column density (i.e. $T \geq 10$ K) and that the emission remains optically thin ($\tau \ll 1$). The first hypothesis is clearly verified (see Fig. 6, upper panel). The optical depth of the H I line is given by:

$$\tau = \frac{3c_{light}^2}{32\pi} \frac{1}{\nu^2} A_{10} N_H \frac{h\nu}{kT} \frac{1}{\Delta\nu} \quad (11)$$

where c_{light} is the velocity of light, A_{10} the spontaneous emission coefficient ($2.8688 \cdot 10^{-15} \text{ s}^{-1}$), N_H the atomic hydrogen column density, h the Planck constant and $\Delta\nu$ the line width. Expressing the line width in km s^{-1} (ΔV) and the column density in cm^{-2} :

$$\tau = 5.50 \cdot 10^{-19} \frac{N_H}{T \Delta V} \quad (12)$$

From Fig. 8, the column density is maximum for $r = 3.72'$ (0.24 pc). Since $T > 160$ K and $\Delta V \sim 3 \text{ km s}^{-1}$, the optical depth is always smaller than 0.03 across the detached shell.

6 DISCUSSION

Our modelling, that assumes stationarity and sphericity, is simplified. However, it allows to grasp the physical conditions within the Y CVn detached shell and already provides a fair adjustment to the high-resolution H I spectra

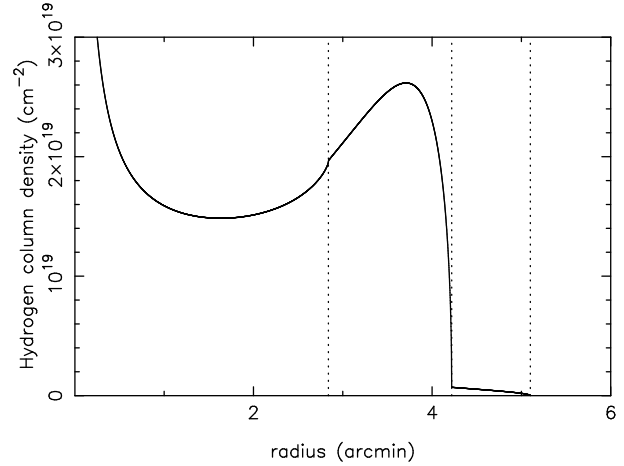


Figure 8. Atomic hydrogen column density in the detached shell model.

Table 2. Model parameters ($d = 218$ pc).

\dot{M} (in hydrogen)	$0.78 \cdot 10^{-7} M_{\odot} \text{ yr}^{-1}$
μ	1.3
t_1	22 500 years
t_{DS}	427 500 years
r_1	0.18 pc (2.84')
r_f	0.27 pc (4.22')
r_2	0.32 pc (5.10')
$T_0 (\equiv T_1^-, T_1^+)$	20 K, 1804 K
$T_f (= T_2)$	167 K
$v_0 (\equiv v_1^-, v_1^+)$	7.8 km s^{-1} , 1.96 km s^{-1}
v_f	0.065 km s^{-1}
v_2	0.9 km s^{-1}
n_1^-, n_1^+	1.0 H cm^{-3} , 3.9 H cm^{-3}
n_f^-, n_f^+	$53. \text{ H cm}^{-3}$, 0.7 H cm^{-3}
n_2	0.5 H cm^{-3}
$M_{r < r_1}$ (in hydrogen)	$1.75 \cdot 10^{-3} M_{\odot}$
$M_{DT,CS}$ (in hydrogen)	$3.32 \cdot 10^{-2} M_{\odot}$
$M_{DT,EX}$ (in hydrogen)	$0.87 \cdot 10^{-3} M_{\odot}$

obtained at different positions with respect to the central star. The fits to some line profiles appear too broad, in particular on the central position (Fig. 2) for which we have the highest signal to noise ratio. However, the total H I flux in the map is, by construction, well reproduced. It could be possible to improve the fits by decreasing the mass loss rate in the model, but this would be at the expense of the agreement with the mass loss rate determined from CO rotational lines, and with the total H I mass.

In Fig. 2 we note a shift in velocity of $\sim 1 \text{ km s}^{-1}$ between the model pedestal and the observed one around 29 km s^{-1} . It comes from the choice in the model of a central velocity at 20.6 km s^{-1} , whereas the stellar velocity is more likely at 21.1 km s^{-1} , as can be estimated from the CO radial velocity (e.g. Knapp et al. 1998). As Comp. 1 is well fitted in velocity, it indicates that the detached shell is on average moving at a velocity of $\sim 0.5 \text{ km s}^{-1}$ with respect to the central star. This could be an effect of a systematic motion of the star with respect to surrounding matter that would exert an asymmetrical pressure on the stellar outflow. This effect, observed along the line of sight, could be related to

the East-West asymmetry observed in our H I map (Fig. 1) and in the ISO image at $90\ \mu\text{m}$ (Izumiura et al. 1996). We note that the Y CVn proper motion towards East (PA = 38° , Sect. 2.1) is consistent with this East-West asymmetry. On the other hand we have presently an indication for a North-South asymmetry that should be investigated with better spatial resolution.

In order to test the assumption that the detached shell of Y CVn is displaced by $1'$ West, we have performed a new modelling of the H I profiles assuming that the source is $1'$ West of the centre of our observation grid, all other model parameters (Table 2) being kept identical. The results are shown in Fig. 9. The intensities $4'$ East and West of Y CVn are well reproduced and the agreement on the central position is even improved. This is an indication that the displacement is real. In that case the hypothesis of sphericity should be re-examined and a non-spherical model (that might also account for the $0.5\ \text{km s}^{-1}$ velocity shift discussed above) should be considered.

A surprising feature of our model is the relatively low density between r_f and r_2 that is not confirmed by the ISO image. As we do not detect any H I emission at $8'$ East and West of Y CVn (Fig. 3, lower panel), we suspect that the outer radius of the H I detached shell has been overestimated by our hypothesis that hydrogen and dust have the same spatial distribution, i.e. that $r_2 = r_{out} = 5.1'$. The displacement of the infrared source West of Y CVn may have led also to an overestimate of r_{out} by Izumiura et al. (1996).

In our model we adopted an empirical temperature profile. Ideally it would have been better to determine the temperature from a cooling function. This would have substantially increased the complexity of our modelling because the temperature enters into the equation of motion (Equ. 5). Also the cooling function is expected to depend on metallicity which is not well constrained for Y CVn. In addition the mean free path of dust particles through the gas should be $\sim 10^9\ \text{cm}$, so that some heating of the gas due to friction should occur, especially close to r_1 where the relative velocity is $\sim 6\ \text{km s}^{-1}$. The grain photoelectric effect may also contribute to heating. The adoption of an empirical profile for the temperature includes all these effects. We note that a shallower profile would have led to a too broad H I emission profile, and that, with a steeper one, the model would have failed to reproduce a correct emission on the East/West position.

The hydrogen mass loss rate that is deduced from the pedestal and from the inner radius of the detached shell is $\sim 0.8\ 10^{-7}\ M_\odot\ \text{yr}^{-1}$. It translates to a total mass loss rate of $\sim 1.0\ 10^{-7}\ M_\odot\ \text{yr}^{-1}$, a value compatible with those derived from CO line fitting. However, as noted in Sect. 2.2, the latter are probably underestimated by a factor 1.4 or more. Considering the uncertainty on the CO abundance, a mass loss rate derived from H I should in principle be more reliable. However we note that our estimate corresponds to an average over $22\ 10^3$ years or even longer. It does not exclude possible variations on smaller timescales. On the other hand the CO estimates correspond to the last period of $\sim 10^3$ years. From a detailed CO modelling Dinh-V-Trung & Nguyen-Q-Rieu (2000) concluded that the Y CVn mass loss rate must have increased by a factor 2 or more over the last 1600 years. Y CVn may thus be presently in an episode

of high mass loss as compared to the average value that we obtained in H I.

In our model of the detached shell we assume that the mass loss rate has been approximately constant for about $4\text{-}5\ 10^5$ years. This may seem too large a duration in view of the expected time between two thermal pulses ($\sim 10^5$ years or less for carbon stars, Straniero et al. 1997). However we noted that Y CVn is a carbon star of the rare J-type and that it may not necessarily be on the TP-AGB. On the other hand the properties that we implicitly assume for the Y CVn outflow fit rather well with the B-type models calculated by Winters et al. (2000) for carbon-rich late-type giants with stellar temperature $\sim 3000\ \text{K}$ and low variability. These models develop stationary outflow structures with no strong temporal variations.

Our H I data modelling confirms that the detached shell of Y CVn is a dense ($\sim 50\ \text{cm}^{-3}$), relatively mild and quiet ($\sim 200\ \text{K}$, $\sim 1\text{-}2\ \text{km s}^{-1}$) region where circumstellar matter stays for at least $4\ 10^5$ years before being mixed with the ISM.

Recently, using far-infrared data from the Spitzer Space Telescope, Ueta et al. (2006) have detected a bow shock nebula with a cometary shape around the AGB star R Hya. Wareing et al. (2006) have modelled this nebula in terms of an interaction of the stellar wind with the surrounding ISM through which R Hya is moving. They estimate the temperature behind the shock at $\sim 35\ 000\ \text{K}$, which corresponds to a star-ISM relative velocity of $\sim 35\ \text{km s}^{-1}$. At such temperature, hydrogen is expected to be entirely ionized.

For Y CVn, although the transverse motions and the radial velocity indicate a motion relative to the ISM of comparable magnitude ($\sim 31\ \text{km s}^{-1}$), we find only a weak evidence for a distortion that could be ascribed to this motion. We cannot exclude the presence of ionized hydrogen between the contact discontinuity, r_f , and the bow shock, r_2 . However, we note that the mass in atomic hydrogen that we estimate from our H I data, $0.04\ M_\odot$, agrees with the total mass estimated from the dust continuum by Izumiura et al. (1996), $\sim 0.06\ M_\odot$. Therefore the detached shell around Y CVn seems to be dominated by compressed neutral matter. Our modelling assumes spherical symmetry, i.e. that the surrounding material is at rest with respect to the central star. This suggests that the external matter, within which the detached shell is expanding, is moving together with Y CVn. This material might therefore not be genuine ISM, but possibly material remaining from an older episode of mass loss. We recall that the stellar evolution models (e.g. Renzini & Fusi Pecci 1988) invoke an important mass loss, perhaps $\sim 0.2\ M_\odot$, on the Red Giant Branch (RGB), that has not been detected up to now. In such a case our way of estimating the mass in the swept-up region (from r_f to r_2), $M_{DT,EX} \sim 0.9\ 10^{-3}\ M_\odot$ in atomic hydrogen (Sect. 4), which relies on the assumption that external matter is interstellar, should be revised. For instance an increase of $M_{DT,EX}$ by a factor 10 ($\sim 0.9\ 10^{-2}\ M_\odot$) would imply a reduction of $M_{DT,CS}$ to $\sim 2.5\ 10^{-2}\ M_\odot$ and a reduction of t_{DS} to $\sim 3.3\ 10^5$ years. This would somewhat change the structure of the detached shell in the model, but not fundamentally.

The phenomenon observed in Y CVn seems different from that leading to the formation of the detached CO shells observed around some carbon stars (Schöier et al. 2005). These molecular shells have a typical radius $\leq 0.1\ \text{pc}$ and

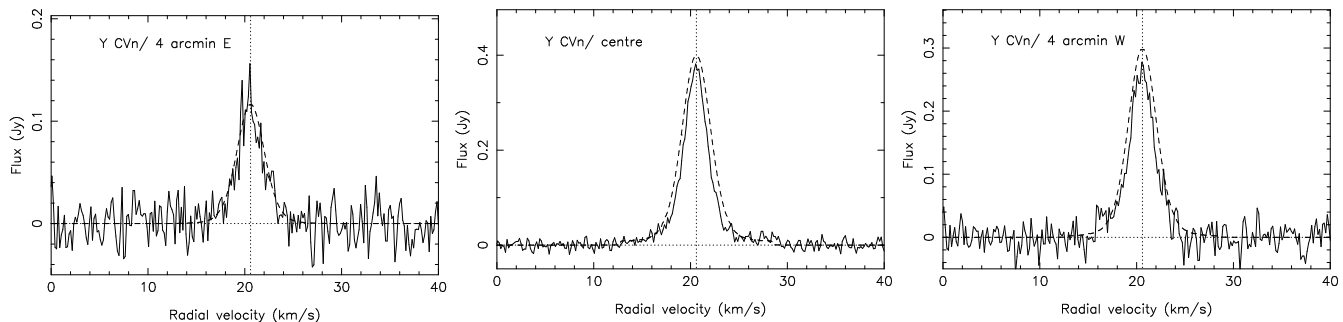


Figure 9. Effect of a shift $1'$ West of the H I source with respect to the centre of the observation grid. Left panel: H I spectrum obtained $4'$ East; centre panel: H I spectrum obtained on the centre; right panel: H I spectrum obtained $4'$ West. The modelled spectra (dashed lines) are discussed in Sect. 6.

are expanding at a velocity $\geq 12 \text{ km s}^{-1}$ (e.g. Olofsson et al. 2000). They are smaller than the Y CVn detached shell (also they look thinner with a CO diameter-to-thickness ratio ~ 5 –10) and do not seem to be slowed down efficiently by an external medium, although there are signs of interaction with a surrounding medium. The sources with CO detached shells show complex CO line profiles with a double-peak (e.g. Olofsson et al. 1990) which is not seen in any of the Y CVn CO spectra (Knapp et al. 1998; Teyssier et al. 2006). Olofsson et al. (1990) have suggested that these CO detached shells are produced by a mass loss eruption, possibly initiated by an He-shell flash. This mechanism is unlikely to play a role for Y CVn, because the central star is probably still on the E-AGB.

The dynamical evolution of the interaction between stellar winds and the ISM has been explored by Villaver et al. (2002). They obtain transient shells ($\sim 20\,000$ years) associated with the wind variations induced by thermal pulses. Longer-lived shells could occur via interaction between successive events of enhanced mass loss, or via the continuous accumulation of ejected material in the interaction region with the ISM. Mattson et al. (2007) have modelled the formation of detached shells around TP-AGB stars. They need to combine an eruption of mass loss to the interaction with external matter in order to explain the properties of CO detached shells. They obtain thin detached shells with small relative thickness ($\Delta R/R \leq 0.01$). From their modelling, the cases for which the observed relative thickness is large ($\Delta R/R \geq 0.1$) may have another origin. Therefore the mechanism for the formation of the Y CVn detached shell might be different from that responsible for the molecular detached shells around carbon stars. Given our low spatial resolution we cannot exclude short time (~ 100 years) fluctuations of the Y CVn mass loss rate such as those found, for instance, for the carbon star IRC +10216 (Mauron & Huggins 2000).

On the other hand, if the scenario that we propose for Y CVn is correct, we expect to find similar detached shells around other AGB stars, and in particular around mass-losing oxygen-rich ones, because there is no reason for it to be specific to carbon stars. From our survey of atomic hydrogen around evolved stars (Paper III) we find H I emission from oxygen-rich as well as from carbon-rich stars. Also the H I line profiles that are observed indicate a slowing-down of circumstellar matter at large distance from the central stars.

7 PROSPECTS

The spatial resolution of our H I data is limited to $\sim 4'$ in RA. Therefore we have used the ISO image at $90 \mu\text{m}$ to better constrain the geometry of the circumstellar shell. On the other hand the high spectral resolution of our H I data has allowed to study directly the kinematics and the physical conditions within the Y CVn detached shell. Also the large collecting area of the NRT has been useful to reach a high sensitivity on the low surface brightness H I emission of Y CVn.

However our interpretation remains limited by the low spatial resolution in H I. For instance, we have used the infrared image as a guide and identified r_1 (H I) with r_{in} (dust) and r_2 with r_{out} . It implicitly assumes that the dust and the gas spatially coincide. Also the infrared emission depends on the dust temperature which should vary with distance to the central star. An imaging in H I would allow to constrain directly the gas density within the shell as a function of the distance to the central star. Indeed in our model we have shown that the optical depth is always smaller than 1 and that the temperature in the detached shell is larger than 10 K, so that the H I emission at each position should be directly proportional to the column density. Therefore interferometric data in H I with a high sensitivity and a high spectral resolution would be very valuable to probe the gas physical conditions and kinematics within the detached shell of Y CVn.

Such high angular resolution imaging in H I should allow to determine clearly r_1 and to compare it to r_{in} . It should also allow to determine the offset of the H I detached shell with respect to Y CVn. The spectrally broad component (2) is expected to be confined to the interior of the gas detached shell, which is expected to be seen only in the spectral bandwidth corresponding to the narrow component (1). Finally, we predict a concentration of hydrogen at $r \sim 0.24 \text{ pc}$ ($3.7'$, see Fig. 8).

Other atomic lines, for instance C I at 492 GHz, might also be valuable tracers of the gas within the detached shell. C I was not detected by Knapp et al. (2000); however, they observed on the stellar position with a beam of only $15''$ and a throw of $60''$ ($< r_1$). In the optical range, resonant lines of Na or K could be useful. Mauron & Guilain (1995) did not detect any Na I/K I emission, but similarly they looked only close to the central star ($5''$).

The conditions for the temperature and the density that

we find in our model might be favorable to the formation of molecular species through a non-equilibrium chemistry as it has been suggested for some regions of the diffuse ISM (Falgarone et al. 2005). In fact as the physical conditions within the detached shell and the timescale can be characterized through modelling, Y CVn could thus be a good target for studying this type of ISM chemistry.

8 CONCLUSIONS

We have presented high spectral resolution H I data obtained on Y CVn with the NRT. The emission is spatially resolved with a diameter $\sim 8' \pm 4'$. The spectrum obtained on the stellar position reveals a rectangular pedestal centered at $+21.1 \text{ km s}^{-1}$ (Comp. 2) that traces an 8 km s^{-1} outflow of $\sim 1.0 \cdot 10^{-7} M_{\odot} \text{ yr}^{-1}$. This outflow corresponds fairly well to the wind detected in the CO rotational lines.

The spectrally narrow component (Comp. 1) is centered at $+20.6 \text{ km s}^{-1}$ and traces an expanding gas shell that we associate with the detached shell imaged by ISO in dust continuum emission at $90 \mu\text{m}$ (Izumiura et al. 1996). The bulk gas temperature within this shell is $\sim 100\text{--}200 \text{ K}$ and the expansion velocity $\sim 1\text{--}2 \text{ km s}^{-1}$. We have developed a simplified model in which the detached shell is produced by a slowing-down of the Y CVn outflow by external matter. In this model the mass loss is taken constant for $\sim 5 \cdot 10^5$ years with the same rate as presently, i.e. $1.0 \cdot 10^{-7} M_{\odot} \text{ yr}^{-1}$. The sharp decrease of the velocity by a factor ~ 4 is interpreted as due to a shock at the inner boundary (termination shock). The Y CVn detached shell thus appears to act as a lock chamber where circumstellar matter is stored for a few 10^5 years before being injected in the ISM.

We note that in our H I model of the detached shell, we have adopted the same dimensions as those of the dust detached shell. These dimensions might not apply exactly and a high angular resolution mapping at 21 cm is needed. It would also provide the exact position of the detached shell with respect to Y CVn.

We find that the surrounding medium which slows down the outflow is almost at rest with respect to Y CVn. Although we cannot exclude that this external medium is local ISM, we suggest that it might rather be made of material left over from an older episode of mass loss, perhaps when the star was on the RGB.

Finally, we caution that the mere presence of a detached shell around an AGB star is not a proof that the central star has undergone an enhanced episode of mass loss. We stress the importance of acquiring high spectral resolution data to complement the dust continuum images obtained in the far-infrared.

ACKNOWLEDGMENTS

The Nançay Radio Observatory is the Unité scientifique de Nançay of the Observatoire de Paris, associated as Unité de Service et de Recherche (USR) No. B704 to the French Centre National de la Recherche Scientifique (CNRS). The Nançay Observatory also gratefully acknowledges the financial support of the Conseil Régional de la Région Centre in France. We thank the referee and L. Matthews for valuable

comments that helped us to improve this paper. We thank Jean Borsenberger for developing a new and efficient procedure for processing NRT data, and Jérôme Pety for his advices in using the GILDAS environment. This research has made use of the SIMBAD database, operated at CDS, Strasbourg, France and of the NASA's Astrophysics Data System.

REFERENCES

- Bergeat J., Knapik A., Rutily B., 2001, A&A, 369, 178
 Bergeat J., Knapik A., Rutily B., 2002, A&A, 390, 967
 Bowers P. F., Knapp G. R., 1988, ApJ, 332, 299
 Dinh-V-Trung, Nguyen-Q-Rieu, 2000, A&A, 361, 601
 Dominy J. F., 1984, ApJS, 55, 27
 Dyson J. E., Williams D. A., 1997, "The physics of the interstellar medium", 2nd edition, Institute of Physics Publishing
 Falgarone E., Hily-Blant P., Pineau des Forêts G., 2005, Proc. "The Dusty and Molecular Universe", A. Wilson (ed.), ESA SP-577, p. 75
 Gardan E., Gérard E., Le Bertre T., 2006, MNRAS, 365, 245 (Paper II)
 Gérard E., 1990, A&A, 230, 489
 Gérard E., Le Bertre T., 2003, A&A, 397, L17
 Gérard E., Le Bertre T., 2006, AJ, 132, 2566 (Paper III)
 Glassgold A. E., Huggins P. J., 1983, MNRAS, 203, 517
 Goebel J. H., et al., 1980, ApJ, 235, 104
 Guandalini R., Busso M., Ciprini S., Silvestro G., Persi P., 2006, A&A, 445, 1069
 Izumiura H., Hashimoto O., Kawara K., Yamamura I., Waters L. B. F. M., 1996, A&A, 315, L221
 Jura M., Kahane C., Omont A., 1988, A&A, 201, 80
 Kahane C., Jura M., 1994, A&A, 290, 183
 Knapp G. R., Crosas M., Young K., Ivezić Ž., 2000, ApJ, 534, 324
 Knapp G. R., Morris M., 1985, ApJ, 292, 640
 Knapp G. R., Pourbaix D., Platais I., Jorissen A., 2003, A&A, 403, 993
 Knapp G. R., Young K., Lee E., Jorissen A., 1998, ApJS, 117, 209
 Lambert D. L., Gustafsson B., Eriksson K., Hinkle K. H., 1986, ApJS, 62, 373
 Lamers J. G. L. M., Cassinelli J. P., 1999, "Introduction to Stellar Winds", Cambridge University Press
 Lattanzio J., Forestini M., 1999, IAUS 191, 31
 Le Bertre T., Gérard E., 2004, A&A, 419, 549 (Paper I)
 Le Bertre T., Gérard E., Winters J. M., 2005, Proc. "The Dusty and Molecular Universe", A. Wilson (ed.), ESA SP-577, p. 217
 Le Bertre T., Matsuura M., Winters J. M., Murakami H., Yamamura I., Freund M., Tanaka M., 2001, A&A, 376, 997
 Matthews L. D., Reid M. J., 2007, AJ, 133, 2291
 Mattsson L., Höfner S., Herwig F., 2007, A&A, in press (arXiv: 0705.2232)
 Maun N., Guilain C., 1995, A&A, 298, 869
 Maun N., Huggins P. J., 2000, A&A, 359, 707
 Neri R., Kahane C., Lucas R., Bujarrabal V., Loup C., 1998, A&AS, 130, 1
 Olofsson H., Bergman P., Lucas R., Eriksson K., Gustafsson B., Bieging J. H., 2000, A&A, 353, 583

- Olofsson H., Carlström U., Eriksson K., Gustafsson B., Willson L. A., 1990, *A&A*, 230, L13
- Perryman M. A. C., et al., 1997, *A&A*, 323, L49
- Renzini A., Fusi Pecci F., 1988, *ARA&A*, 26, 199
- Schöier F. L., 2007, Proc. “*Why Galaxies Care About AGB Stars*”, F. Kerschbaum, C. Charbonnel & R. Wing (eds.), ASP Conf. Ser., in press
- Schöier F. L., Lindqvist M., Olofsson H., 2005, *A&A*, 436, 633
- Schöier F. L., Olofsson H., 2000, *A&A*, 359, 586
- Schöier F. L., Ryde N., Olofsson H., 2002, *A&A*, 391, 577
- Sfeir D. M., Lallement R., Crifo F., Welsh B. Y., 1999, *A&A*, 346, 785
- Straniero O., Chieffi A., Limongi M., Busso M., Gallino R., Arlandini C., 1997, *ApJ*, 478, 332
- Teyssier D., Hernandez R., Bujarrabal V., Yoshida H., Phillips T. G., 2006, *A&A*, 450, 167
- Ueta T., Speck A. K., Stencel R. E., et al., 2006, *ApJ*, 648, L39
- van Loon J. Th., 2007, Proc. “*Why Galaxies Care About AGB Stars*”, F. Kerschbaum, C. Charbonnel & R. Wing (eds.), ASP Conf. Ser., in press
- Villaver E., García-Segura G., Manchado A., 2002, *ApJ*, 571, 880
- Wareing C. J., Zijlstra A. A., Speck A.K., et al., 2006, *MNRAS*, 372, L63
- Winters J. M., Le Bertre T., Jeong K. S., Helling Ch., Sedlmayr E., 2000, *A&A*, 361, 641
- Young K., Phillips T. G., Knapp G. R., 1993a, *ApJS*, 86, 517
- Young K., Phillips T. G., Knapp G. R., 1993b, *ApJ*, 409, 725